Green Chemistry

PAPER

View Article Online
View Journal | View Issue



Cite this: *Green Chem.*, 2015, **17**, 2426

# Towards the sustainable production of pyridines *via* thermo-catalytic conversion of glycerol with ammonia over zeolite catalysts†

Lujiang Xu, Zheng Han, Qian Yao, Jin Deng, Ying Zhang,* Yao Fu* and Qingxiang Guo

Received 15th November 2014,
Accepted 26th January 2015

DOI: 10.1039/c4gc02235a

www.rsc.org/greenchem

In this study, renewable pyridines could be directly produced from glycerol and ammonia *via* a thermo-catalytic conversion process with zeolites. The major factors, including catalyst, temperature, weight hourly space velocity (WHSV) of glycerol to catalyst, and the molar ratio of ammonia to glycerol, which may affect the pyridine production, were investigated systematically. The optimal conditions for producing pyridines from glycerol were achieved with HZSM-5 (Si/Al = 25) at 550 °C with a WHSV of glycerol to catalyst of 1 $h^{-1}$ and an ammonia to glycerol molar ratio of 12 : 1. The carbon yield of pyridines was up to 35.6%. The addition of water to the feed decreased the pyridine yield, because water competed with glycerol on the acid sites of the catalyst and therefore impacted the acidity of the catalyst. After five reaction/regeneration cycles, a slight deactivation of the catalyst was observed. The catalysts were investigated by $N_2$ adsorption/desorption, XRD, XRF and $NH_3$-TPD and the results indicated that the deactivation could be due to the structure changes and the acid site loss of the catalyst. The reaction pathway from glycerol to pyridines was studied and the main pathway should be that glycerol was initially dehydrated to form acrolein and some by-products such as acetaldehyde, acetol, acetone, *etc.*, and then acrolein, a mixture of acrolein and acetaldehyde, or other by-products reacted with ammonia to form imines and finally pyridines.

## Introduction

The pyridine substructure is one of the most prevalent heterocycles found in natural products, pharmaceuticals, and functional materials.[1,2] Pyridines (pyridine, 2-methylpyridine, 3-methylpyridine and 4-methylpyridine) are widely used as building blocks for the synthesis of agrochemicals and pharmaceuticals due to their high chemical activity and biological activity. They have also been used as solvents as well as catalysts in the chemical industry.[3,4] Traditionally, pyridines were produced from coal tar as a by-product of the coal gasification. Pyridines produced by this method could not meet the increasing demand of the market, which resulted in the development of alternative synthetic methods of pyridines from acyclic molecules (carbonyls, dicarbonyls, dicyano alkanes, alkenes, and alkynes) over zeolites (HZSM-5, HY and H-β).[5–9] Formaldehyde, acetaldehyde and acrolein are used to produce pyridines industrially. However, these feedstocks are non-renewable fossil based materials. In industry, formaldehyde is produced by the catalytic oxidation of methanol.[10] Acetaldehyde is mainly produced by the oxidation of ethylene *via* the Wacker process.[11] Acrolein is prepared by oxidation of propene.[12] The chemical properties of these aldehydes are unstable and prone to aggregation. Furthermore, formaldehyde and acrolein are highly toxic and carcinogenic.[13,14] Therefore, it would be highly desirable to find a renewable and environment friendly feedstock to produce pyridines on the large scale.

Glycerol, as a co-product in the production of biodiesel by transesterification of vegetable oils or animal fats, is a potentially desired candidate. About 1 kg of crude glycerol is generated for every 9 kg of biodiesel produced.[15] Recently, glycerol has a remarkable production increase because of the demand and the production boosts of biodiesel. The anticipated production of glycerol will be 1.54 million tonnes in 2015.[16,17]

*Collaborative Innovation Center of Chemistry for Energy Materials, Anhui Province Key Laboratory of Biomass Clean Energy, Department of Chemistry, University of Science and Technology of China, Hefei, Anhui, China.*
*E-mail: zhzhying@ustc.edu.cn, fuyao@ustc.edu.cn; Fax: (+86) 551-6360-6689*

† Electronic supplementary information (ESI) available: The scheme of the fixed bed reactor for glycerol conversion; $NH_3$-TPD spectra of the catalysts; the liquid product distribution of glycerol dehydration over zeolites with nitrogen. See DOI: 10.1039/c4gc02235a

However, because the market demand for glycerol is far less than its production, the market price of glycerol has decreased rapidly from around 1200 USD per ton in 2000 to 400 USD per ton in 2010.[18] Such an inexpensive feed calls for the development of processes for the conversion of glycerol into other value-added chemicals.

Compared with the aldehydes which are used to produce pyridines, glycerol is renewable, nontoxic and chemically stable. Therefore, utilizing glycerol for pyridine production could have a tremendous technical impact. More than sixty years ago, Cullinane *et al.* mentioned the formation of pyridine and derivatives by reacting ammonia, urea or ammonia salts with glycerol for about 10 hours, but the selectivity and yield of pyridine were too low to be applied in industry.[19] Acrolein is an important intermediate in the production of pyridines from formaldehyde and acetaldehyde. Many literature papers have reported that acrolein could be produced from glycerol *via* a catalytic gas phase dehydration process.[16,20–29] The recent development of glycerol to acrolein over different acid catalysts, such as zeolites, metal oxides, and heteropolyacids (HPAs) supported on metal oxides, and the effects of catalyst pore structure and acid properties on the dehydration of glycerol have been reviewed and well documented.[16,20,21] Dubois *et al.* synthesized pyridines by a two-step method that included: (1) glycerol dehydration to acrolein, acrolein enrichment and separation, and (2) reaction of the acrolein from the preceding step with the additional acetaldehyde to form pyridines.[30] Gullu *et al.* synthesized pyridines from glycerol and inorganic ammonium salts *via* micro-assisted pyrolysis.[31]

In this study, zeolite catalysts were employed to convert glycerol into pyridines in one step *via* the thermo-catalytic conversion process. Ammonia served as both a carrier gas and a reactant. Different catalysts, MCM-41, β-zeolite, ZSM-5 (Si/Al = 50) and HZSM-5 with different Si/Al ratios (Si/Al = 25, 50, 80), were screened. The major factors, including catalyst, reaction temperature, WHSV of glycerol to catalyst, the molar ratio of ammonia to glycerol and water content in the feeding solution, were investigated systematically. The stability of the catalyst was tested by five reaction/regeneration cycles. The catalyst of each cycle was characterized by $N_2$ adsorption/desorption, X-ray diffraction (XRD), X-ray fluorescence (XRF), and temperature programmed desorption of ammonia ($NH_3$-TPD) analyses. The reaction pathway was also investigated.

# Experimental section

## Materials

Ethanol (≥99.5, AR) and glycerol (≥99.5, AR) were purchased from Sinopharm Chemical Reagent Co. Ltd. Pyridine (≥99.5, AR), 2-methylpyridine (≥99.5, AR), 3-methylpyridine (≥99.5, AR), and bi-cyclohexane (≥99.5, AR) were purchased from Aladin Chemical Reagent Co. Ltd. All these chemicals were used as received. $NH_3$ (≥99.995, AR), $N_2$ (99.999%), Ar (99.999%), He (99.999%) and standard gas were purchased from Nanjing Special Gases Factory.

Table 1 Typical properties of the catalysts

| Catalyst | BET surface area ($m^2\ g^{-1}$) | Pore diameter (nm) | Si/Al | Total acid ($\mu mol\ g^{-1}$) |
|---|---|---|---|---|
| β-Zeolite | 640 | 0.7 | 50 | 683.3 |
| MCM-41 | 1000 | 3.8 | 50 | 260.0 |
| ZSM-5 | 420 | 0.5 | 50 | 255.5 |
| HZSM-5-1 | 350 | 0.5 | 50 | 293.6 |
| HZSM-5-2 | 370 | 0.5 | 25 | 580.6 |
| HZSM-5-3 | 375 | 0.5 | 80 | 92.4 |

## Catalysts and characterization

MCM-41, β-zeolite, ZSM-5 (Si/Al = 50) and HZSM-5 with different Si/Al ratios (Si/Al = 25, 50, 80) were purchased from the Catalyst Plant of Nankai University. The typical properties of these catalysts are shown in Table 1. The particle size of the catalysts was about 40 meshes.

The XRD patterns were analyzed using a RigakuD/MAX-2500 diffractometer in a $2\theta$ range of 5–80° (with a $2\theta$ step of 0.02°) using Cu Kα radiation ($k$ = 1.5406 Å). The $N_2$ adsorption/desorption isotherms of the catalysts were measured at −196 °C using the COULTER SA 3100 analyzer. The surface area of the catalyst was calculated by the Brunauer–Emmett–Teller (BET) method. The Si/Al ratio of zeolites was measured by XRF (Shimadzu Corporation, Japan). The data were analyzed using the semi-quantitative program UniQuant.

For the $NH_3$-TPD tests, about 200 mg of sample were put in a reactor and pre-treated *in situ* for 1 h at 500 °C under a flow of argon. After cooling to 90 °C, ammonia adsorption was performed by feeding pulses of reactant grade ammonia (>99.995%) to the reactor using a flow of dry argon (>99%) of 60 ml $min^{-1}$. After the catalyst surface became saturated, the sample was kept at 90 °C for 2 h to remove the ammonia. Ammonia was thermally desorbed by rising the temperature with a linear heating rate of approximately 8 °C $min^{-1}$ from 90 °C to 700 °C. The amount of desorbed $NH_3$ was measured using a gas chromatograph (GC-SP6890, Shandong Lu-nan Ruihong Chemical Instrument Co., Ltd, Tengzhou China) with a thermal conductivity detector (TCD).

## Apparatus for thermo-catalytic conversion of glycerol over zeolites to pyridines

As shown in Fig. S1,† a bench-top continuous flow reactor consisting of a quartz tube reactor heated by a furnace and a condensation tube bathed in liquid nitrogen was used for these experiments. The catalyst bed supported by quartz wool was built up in the heating zone of the reactor. The liquid feed was fed into the reactor with a peristaltic pump under a certain flow rate and purged with ammonia. Volatile products were trapped in the condensation tube cooled with liquid $N_2$.

## Product analysis

The liquid produced was analyzed by GC-MS (Thermo Trace GC Ultra with an ISQ i mass spectrometer) equipped with a TR-35MS capillary column (30 m × 0.25 mm × 0.25 mm). Split injection was performed at a split ratio of 50 using helium

(99.999%) as a carrier gas. The GC heating ramp was: (1) hold at 40 °C for 3 min, (2) heat to 180 °C at 5 °C $min^{-1}$, (3) heat to 280 °C at 10 °C $min^{-1}$, and (4) hold at 280 °C for 5 min.

The total amount of liquid products was determined by the weight difference of the condensation tube before and after the experiment. The coke at the end of the run was measured after the reaction by weighing the catalyst. The carbon yield of coke was further determined by elemental analysis.

The glycerol and major liquid products were quantified by gas chromatography (GC 1690, Kexiao, China) employing a 30 m × 0.25 mm × 0.25 μm fused-silica capillary column (HP-Innowax, Agilent). The liquid sample was mixed with bicyclohexane as the internal standard and diluted by ethanol. The GC operating conditions were as follows: carrier gas: nitrogen; injection port: 250 °C in a split mode; detector (FID): 250 °C; heating ramp: heating up from 40 °C to 250 °C at a rate of 10 °C $min^{-1}$, and holding at a final temperature for 5 min.

The gas products were analyzed by collecting the gas in gas bags. The gas bags were weighed before and after reaction and their contents were analyzed using gas chromatography (GC-SP6890, Shandong Lu-nan Ruihong Chemical Instrument Co., Ltd, Tengzhou, China) with two detectors, a TCD for the analysis of $H_2$, CO, $CH_4$, and $CO_2$ separated on a TDX-01 column, and a FID (flame ionization detector) for gas hydrocarbons separated on a Porapak Q column. The moles of gas products were determined by the normalization method with standard gas.

The conversion of glycerol, the yield of coke, gases, pyridines and aromatics, and the selectivity of pyridines and gases were calculated from eqn (1)–(7).

$$\text{Glycerol conversion}\,(\%) = \frac{\text{Moles of glycerol reacted}}{\text{Moles of glycerol fed}} \times 100\% \quad (1)$$

$$\text{Coke yield}\,(\text{C}\%) = \frac{\text{Moles of carbon in solid residue}}{\text{Moles of carbon in glycerol fed}} \times 100\% \quad (2)$$

$$\text{Gases yield}\,(\text{C}\%) = \frac{\text{Carbon moles in gases}}{\text{Moles of carbon in glycerol fed}} \times 100\% \quad (3)$$

$$\text{Pyridine yield}\,(\text{C}\%) = \frac{\text{Moles of carbon in Pyridines}}{\text{Moles of carbon in glycerol fed}} \times 100\% \quad (4)$$

$$\text{Aromatics yield}\,(\text{C}\%) = \frac{\text{Moles of carbon in aromatics}}{\text{Moles of carbon in glycerol fed}} \times 100\% \quad (5)$$

$$\text{Pyridine selectivity}\,(\%) = \frac{\text{Moles of carbon in specific pyridine}}{\text{Total moles of carbon in all pyridines}} \times 100\% \quad (6)$$

$$\text{Gas selectivity}\,(\%) = \frac{\text{Moles of carbon in specific gas}}{\text{Total moles of carbon in gases identified}} \times 100\% \quad (7)$$

## Results and discussion

### Catalyst property effect on glycerol conversion with ammonia

The appropriate catalyst was essential to selectively obtain target products in the thermo-catalytic conversion process. Six catalysts with different properties were tested in this study. The typical properties of these catalysts are shown in Table 1. Table 2 summarizes the detailed results of thermo-catalytic conversion of glycerol over different zeolites at 500 °C. It can be seen that the products from thermo-catalytic conversion of glycerol were coke, gases, pyridines and a little aromatics. The detected gases were CO, $CH_4$, $C_2H_4$ and $C_3H_6$. A trace amount of $CO_2$ was also produced during this process, because when the gases passed through the $Ca(OH)_2$ solution, a very small amount of white precipitant could be observed. However, $CO_2$ was difficult to be detected by GC due to its reaction with ammonia to form ammonium carbonate. Since the amount of $CO_2$ was small and it was hard to give accurate data, we did not report it in Table 2.

As shown in Table 2, when there was no catalyst, the conversion of glycerol was only 5.6%. Gases and coke were the major products, and only trace amounts of pyridines (below 1% carbon yield) were detected in the liquids. Then, three kinds of catalysts, β-zeolite, MCM-41 and ZSM-5, with different acid contents and pore structures were screened firstly. When these zeolites were introduced, glycerol was almost completely converted and the conversion of glycerol increased to nearly 100%. Compared with β-zeolite and MCM-41, more pyridines were produced using ZSM-5, and the carbon yield reached about 20%. The kinetic diameter of pyridines was about 0.585 nm, which was similar to the pore diameter of ZSM-5.[5,32] ZSM-5 consisted of two perpendicularly intersecting channels. The larger one has a near circular pore structure with dimensions of 0.54 × 0.56 $nm^2$, and the smaller channels have a geometry of 0.51 × 0.54 $nm^2$. The intersection of these channels which contains the proposed active site is an approximately 0.9 nm cavity.[33] More coke and less pyridines were produced using β-zeolite. Although β-zeolite has intersecting channels similarly to ZSM-5, this zeolite is a mixture of three polymorphs, which is different from ZSM-5.[34] Furthermore, as shown in Table 1, the total acid content of β-zeolite was up to 683.3 μmol $g^{-1}$, which was much more than for ZSM-5. Thus, more coke was produced in the thermo-catalytic conversion of glycerol over the β-zeolite process. Compared with ZSM-5, more gases and coke and less pyridines were produced using MCM-41. The acid content of MCM-41 was similar to ZSM-5. The difference in the product distribution may be caused by the different structures between ZSM-5 and MCM-41. MCM-41 possesses hexagonally packed arrays of channels with a pore diameter of around 3.8 nm, which has no shape selectivity to pyridines.[35,36]

 

Table 2 Thermo-catalytic conversion of glycerol with ammonia over various catalysts[a]

| Entry | 1 | 2 | 3 | 4 | 5 | 6 | 7 |
|---|---|---|---|---|---|---|---|
| Catalyst | Blank | β-Zeolite | MCM-41 | ZSM-5 | HZSM-5-1 | HZSM-5-2 | HZSM-5-3 |
| Si/Al | — | 50 | 50 | 50 | 50 | 25 | 80 |
| Glycerol conversion[b] (%) | 5.6 | 92.6 | 100 | 100 | 100 | 100 | 100 |
| Overall carbon yield[c] (C %) | | | | | | | |
| Coke | 20.7 | 30.1 | 19.4 | 13.7 | 13.0 | 13.2 | 14.5 |
| Gases | 41.8 | 47.3 | 54.3 | 53.6 | 52.7 | 47.5 | 50.9 |
| Pyridines | — | 15.3 | 9.7 | 19.2 | 22.8 | 26.0 | 20.9 |
| Aromatics | — | 0.5 | 0.3 | 0.4 | 0.6 | 0.9 | 0.4 |
| Pyridine selectivity (%) | | | | | | | |
| Pyridine | — | 63.8 | 66.4 | 71.1 | 69.3 | 67.3 | 72.3 |
| 2-Methylpyridine | — | 10.5 | 11.0 | 11.1 | 12.1 | 10.0 | 8.8 |
| 3-Methylpyridine | — | 24.1 | 21.5 | 16.8 | 17.9 | 21.4 | 16.1 |
| 4-Methylpyridine | — | 1.6 | 1.1 | 2.0 | 1.7 | 1.3 | 2.8 |
| Other alkylpyridines | — | <1 | <1 | <1 | <1 | <1 | <1 |
| Gases selectivity (%) | | | | | | | |
| CO | 85.1 | 71.2 | 69.9 | 70.1 | 78.8 | 80.3 | 76.4 |
| $CH_4$ | 5.9 | 5.8 | 8.6 | 5.9 | 6.4 | 5.3 | 7.2 |
| $C_2H_4$ | 3.5 | 13.0 | 15.3 | 15.5 | 12.3 | 11.9 | 14.0 |
| $C_3H_6$ | 1.5 | 9.0 | 6.2 | 8.5 | 2.5 | 2.5 | 2.4 |

[a] Reaction conditions: reaction temperature, 500 °C; HZSM-5, Si/Al = 25, 1 g; WHSV, 1 $h^{-1}$; $NH_3$ to glycerol molar rate, 8 : 1; glycerol content, 100%. [b] Mole conversion: mol%. [c] Carbon yield: carbon mol%.

Usually, acid is an important factor to influence the product distribution. Converting ZSM-5 to HZSM-5 can introduce acid to the catalyst but keep its pore structure; therefore, HZSM-5/1 with the same Si/Al ratio (50) as ZSM-5 was selected to investigate the acid effect. Compared to the results in Table 2, entries 4 and 5, the introduction of acid slightly changed the coke and gas production. However, it increased the pyridine yield from 19.2% to 22.8%. Since the alumina contents of the zeolite determine the acid site densities of the catalyst which may influence the product distribution, two other HZSM-5 samples with silica to alumina ratios of 25 and 80 were also tested in this study. The total acid contents of these catalysts determined by $NH_3$-TPD are shown in Table 1, and the detailed information can be seen in ESI (Fig. S2†). The acid density decreased with the increase of the Si/Al ratio. As shown in Table 2, entries 5–7, with the increase of the Si/Al ratio from 25 to 80, the yield of pyridines decreased, and HZSM-5-2 (Si/Al = 25), which possesses the highest acid concentration, resulted in the highest pyridine yield among all the catalysts and the yield of pyridines reached about 26%. Therefore HZSM-5 (Si/Al = 25) was selected as the optimal catalyst in the following study.

### The effect of temperature on the pyridine production from glycerol

The temperature effect on the glycerol conversion with ammonia was investigated in the temperature range of 300 to 600 °C. As shown in Fig. 1a, the yield of coke decreased and the yield of gases increased with increasing temperature. The conversion of glycerol increased from 68.2% to 100% from 300 to 450 °C, and the pyridine yield also increased from 3.2% to 23.3%. The highest yield of pyridines (32.1%) was obtained at about 550 °C. If the temperature was increased to 600 °C, the yield of pyridines decreased to 8.1%. Meanwhile, the yield of aromatics increased from 2.2 to 15.9%. It indicated that the temperature at around 550 °C is in favor of pyridine production.

Fig. 1b shows the effect of reaction temperature on the pyridine selectivity. Pyridine and 3-methylpyridine are the major products. Meanwhile, a small amount of 2-methylpyridine and a trace amount of 4-methylpyridine were also produced. With temperature increasing from 300 to 600 °C, the pyridine selectivity increased from 58% to 75.1% and the 4-methylpyridine selectivity increased from 0.6% to 3.7%. The 3-methylpyridine selectivity decreased from 32.7% to 12.2%. The selectivity of 2-methylpyridine showed no regularity in the entire temperature range. The pyridine distribution change could be explained by previous findings. Pyridine is most likely formed from the reaction of acrolein and acetaldehyde with ammonia, 3-methylpyridine is the major product from the reaction of acrolein with ammonia, 2-methylpyridine is mainly formed from the reaction of acrolein and acetone with ammonia, and 4-methylpyridine was from the reaction of acetaldehyde with ammonia.[6] With temperature increasing, the cracking reaction of glycerol became severe, and more acetaldehyde as the by-product would be produced in the glycerol dehydration process, while there is nearly no change in the acetone production.[22] As a result of the above reasons, as the temperature increased, the selectivity of pyridine and 4-methylpyridine increased but 3-methylpyridine decreased significantly.

Fig. 1c shows the effect of temperature on the gas product distribution. The main products detected in the gas phase were CO and some olefins. The CO selectivity decreased but $CH_4$ and $C_2H_4$ selectivity increased with temperature. No $C_3H_6$ was detected when the reaction temperature was lower than 450 °C. At higher temperature, the selectivity of $C_3H_6$ was constant at 3%. At a lower temperature, side reactions in this

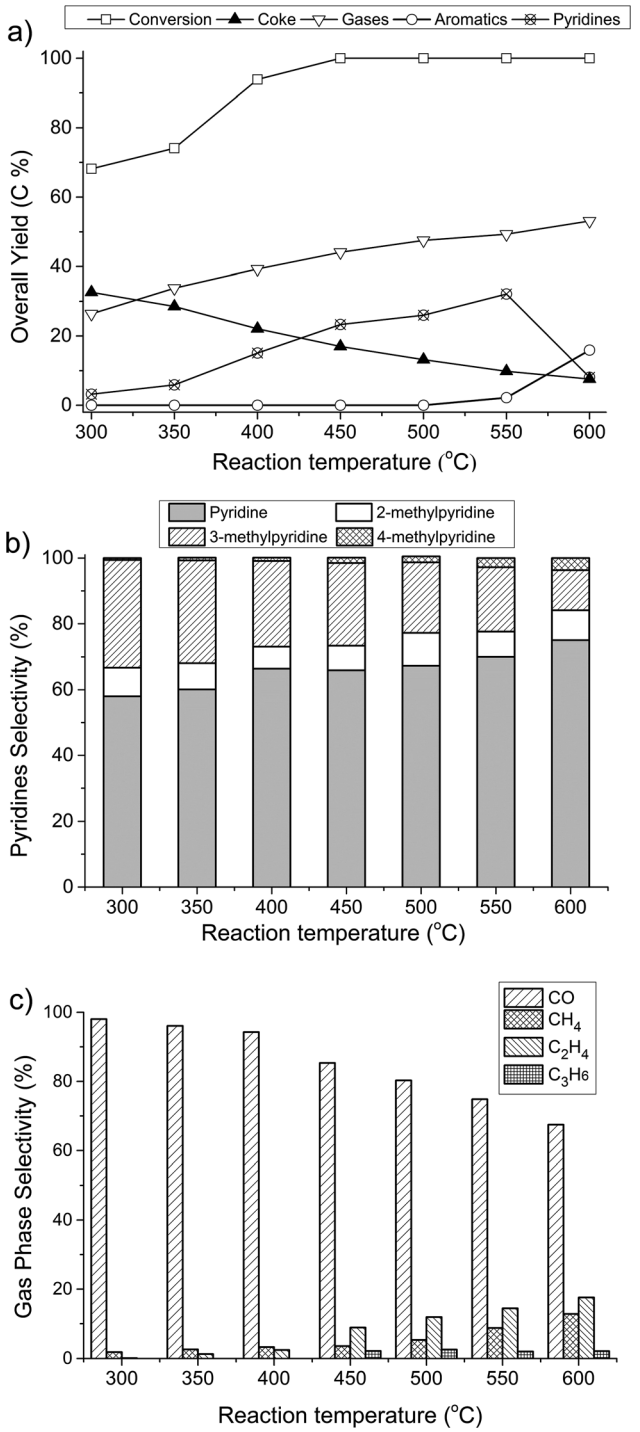


**Fig. 1** The effect of the reaction temperature on the overall yield (a), pyridine selectivity (b), the gas selectivity (c) obtained *via* thermo-catalytic conversion of glycerol. (Reaction conditions: catalyst, HZSM-5, Si/Al = 25; catalyst usage, 1 g; glycerol feed rate, 1 ml $h^{-1}$; $NH_3$ flow rate, 40 ml $min^{-1}$; glycerol content, 100%.)

process were not notable and the product distribution of gases was simple, while at a higher temperature, the side reactions such as cracking, decarbonylation, and oligomerization become more significant. Thus the selectivity of olefins and hydrocarbons increased with the increase of temperature.

### The effect of WHSV of glycerol to catalyst on the pyridine production

The WHSV was defined as the ratio of the mass flow rate of glycerol to the mass of catalyst used for the reaction. During the experiments, the mass flow rate of glycerol ranged from 0.5–2 g $h^{-1}$ while the mass of catalyst was kept constant at 1 g. Fig. 2 shows the glycerol conversion, the overall yield of coke, gases, pyridines, aromatics and the selectivity of pyridines as a function of the WHSV. When the WHSV was less than 1 $h^{-1}$, the conversion of glycerol was 100%, and then when the WHSV was increased from 1 to 2 $h^{-1}$, the conversion of glycerol decreased from 100% to 73.8%. With the increase of WHSV, the carbon yield of coke, gases and aromatics decreased from 10.7% to 7.6%, 52.9% to 40.6%, and 3.7% to 1.4%, respectively. The pyridine yield firstly increased from 27.8% to 35.6% as the WHSV increased from 0.5 to 1 $h^{-1}$, and then decreased gradually to 23.7% as the WHSV further increased to 2 $h^{-1}$. A lower WHSV would result in overreaction of the glycerol over the catalyst which caused the yield of pyridines to decrease and the yield of gases and coke to increase. A higher WHSV would lead to the incomplete reaction of glycerol over the catalyst and the conversion of glycerol

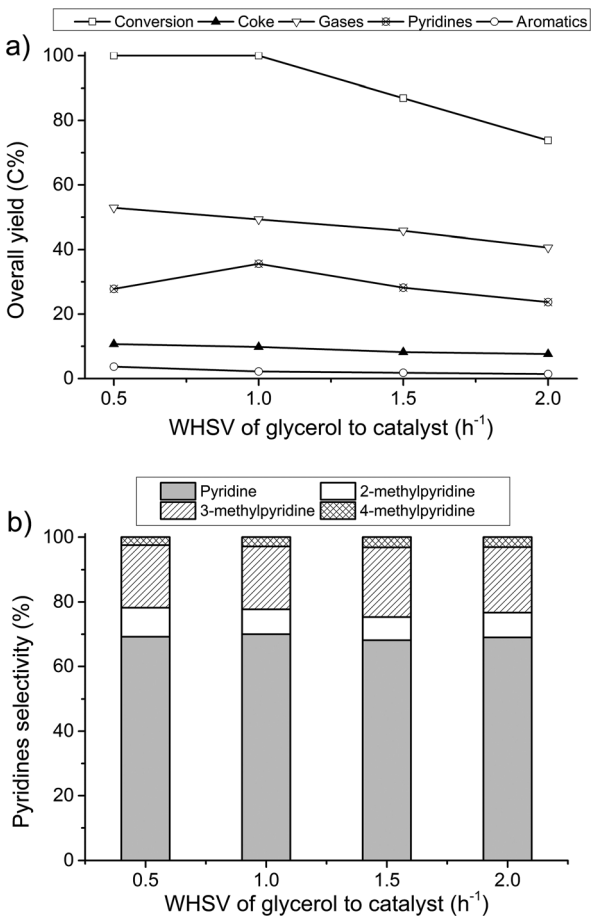


**Fig. 2** The effect of WHSV of glycerol to catalyst on the pyridines distribution, (a) overall yield, (b) pyridine selectivity. (Reaction conditions: 550 °C; HZSM-5, Si/Al = 25, 1 g; $NH_3$ to glycerol molar ratio, 12 : 1; glycerol content, 100%.)

 

decreased. As shown in Fig. 2b, as the WHSV increased from 0.5 to 2 $h^{-1}$, the distributions of pyridines had almost no change. The main products of pyridines were pyridine and 3-methylpyridine, and their selectivity was kept at about 70% and 20%, respectively. Meanwhile, the selectivity of by-products 2-methylpyridine and 4-methylpyridine was also kept at about 8% and 3%, respectively. Thus, the optimal WHSV of glycerol to catalyst for producing pyridines was about 1 $h^{-1}$, and the yield of pyridines was about 35.6%.

### The effect of ammonia to glycerol molar ratio on the pyridine production

The effect of the ammonia to glycerol molar ratio on glycerol thermo-catalytic conversion to pyridines was investigated by fixing the WHSV of glycerol to catalyst at 1 $h^{-1}$ and the mass of catalyst at 1 g while changing the flow rate of ammonia. The molar ratio of ammonia to glycerol was in the range from 4 : 1 to 20 : 1. In this study, the ammonia served not only as the reagent but also as the carrier gas. Different ammonia to glycerol molar ratios would result in different reaction times of glycerol and the pyrolytic vapor in the system. As shown in Fig. 3a, with the molar ratio of ammonia to glycerol rising from 4 : 1 to 20 : 1, the conversion of glycerol was kept at 100%, and the total carbon yield of the detected products was above 90%. The coke yield decreased from 14.1% to 8.8%, while the gas yield increased from 45.2% to 55.9%. The carbon yield of aromatics was very low and was kept at about 2%. During this process, a higher ammonia to glycerol ratio corresponded to a higher ammonia flow rate, which could cause the reaction time of the feedstock stream over catalyst to decrease, which could cause the reaction from glycerol to pyridines insufficient. In contrast, a lower ammonia to glycerol ratio corresponded to a lower ammonia flow rate, which could cause the reaction time of the feedstock stream over catalyst to increase, and led to further reaction of pyridines. When the molar ratio of ammonia to glycerol was 12 : 1, the yield of pyridines reached 35.6%. Fig. 3b shows that the major product distribution in pyridines did not change significantly, and the main products were still pyridine and 3-methylpyridine. The selectivities of pyridine, 2-methylpyridine, 3-methylpyridine and 4-methylpyridine were about 70%, 8%, 20% and 2%, respectively.

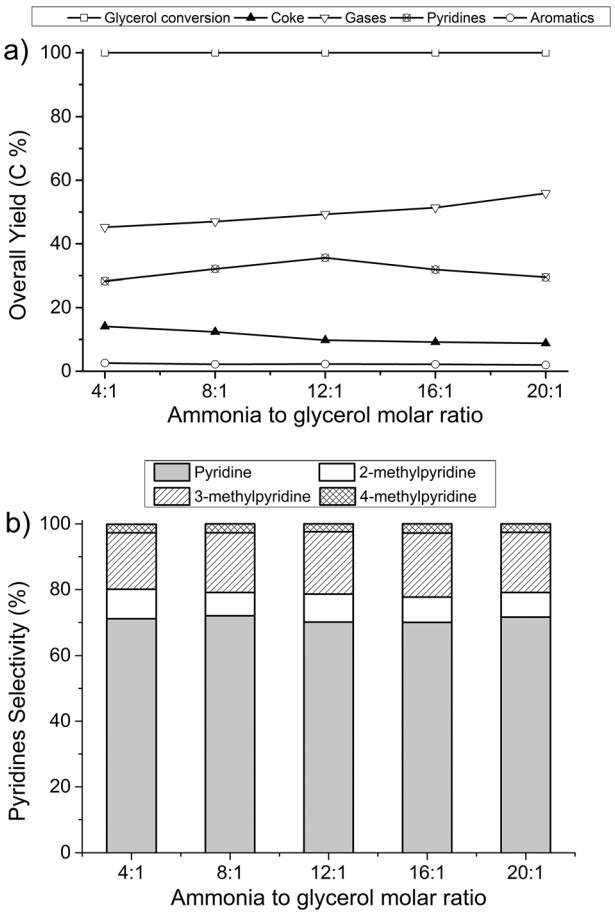


Fig. 3 The product distribution and the pyridine selectivity obtained from thermo-catalytic conversion of glycerol with different ammonia to glycerol molar ratios, (a) overall yield; (b) pyridine selectivity. (Reaction conditions: 550 °C; HZSM-5, Si/Al = 25, 1 g; WHSV, 1; glycerol content, 100%.)

### The effect of water content of a glycerol–water solution on the pyridine production

Crude glycerol obtained from biodiesel production usually contains a lot of water, which can influence the product distribution and the acrolein yield in the glycerol gas phase dehydration process.[23] In this study, glycerol gas phase dehydration is an essential process which may influence the yield and selectivity of pyridines. Experiments on thermo-catalytic conversion of glycerol–water solution with different water contents were carried out. Table 3 shows the effect of water content in the solution on the pyridine production. The pyridine yield decreased from 35.6% to 28.5% with the water content in the feed increased from 0 to 80%. Meanwhile, the selectivity of pyridine increased from 70.7 to 78.2%. There was a slight decrease of the selectivity to 2-methylpyridine and 3-methylpyridine with increasing water content. Based on Table 2, the acidity of the catalyst is an important factor for producing pyridines in the thermo-catalytic conversion of glycerol with the

Table 3 The effect of water content in the glycerol–water solution on the yield and selectivity on the pyridine production[a]

| Entry | 1 | 2 | 3 | 4 | 5 |
|---|---|---|---|---|---|
| Water content (wt%) | 0 | 20 | 40 | 60 | 80 |
| Overall carbon yield[b] (C %) | | | | | |
| Coke | 9.8 | 9.3 | 8.5 | 7.3 | 6.4 |
| Gases | 49.3 | 49.3 | 51.6 | 52.7 | 56.8 |
| Pyridines | 35.6 | 34.5 | 34.7 | 29.9 | 28.5 |
| Aromatics | 2.2 | 2.2 | 2.4 | 2.5 | 2.6 |
| Pyridine selectivity (%) | | | | | |
| Pyridine | 70.7 | 70.2 | 71.0 | 75.5 | 78.2 |
| 2-Methylpyridine | 8.6 | 8.1 | 7.9 | 5.8 | 3.5 |
| 3-Methylpyridine | 17.8 | 18.7 | 18.2 | 16.2 | 16.1 |
| 4-Methylpyridine | 2.9 | 3.0 | 2.9 | 2.5 | 2.2 |
| Other alkylpyridines | <1 | <1 | <1 | <1 | <1 |

[a] Reaction conditions: reaction temperature, 550 °C; catalyst, HZSM-5, Si/Al = 25; catalyst usage, 1 g; $NH_3$ flow rate, 60 ml $min^{-1}$, glycerol content, 100%. [b] Carbon yield: carbon mol%.

ammonia process. Because water competes with glycerol on the acid sites of the catalyst[23] and therefore impacts the acidity of the catalyst, it is intelligible that the pyridine yield decreases with increasing the water content. Furthermore, it was found that the selectivity of acrolein and acetaldehyde increased and the selectivity of acetone decreased with increasing water content.[22,23] As mentioned previously, pyridine is mainly formed by acrolein and acetaldehyde, and 2-methylpyridine is mainly formed by acrolein and acetone.[3,4] Thus, the selectivity of pyridine increased and the selectivity of 2-methylpyridine decreased with increasing the water content.

### Catalyst stability study

To study the stability of the catalyst during the thermo-catalytic conversion of glycerol with ammonia, five reaction/regeneration cycles of catalyst were conducted. For each cycle, the reaction was performed with a WHSV of 1 $h^{-1}$ at 550 °C for 1 h. After the reaction, the spent catalyst was regenerated in an air stream at 600 °C for 3 hours to remove the coke. As shown in Fig. 4, after using 5 times, the yield of pyridines decreased from 35.6% to 30.3%, while the yields of gases and coke increased from 49.3% to 52.6% and 9.8% to 13.0%, respectively. The yield of aromatics did not change a lot and remained at around 2.5%. Based on these results the catalyst was slightly deactivated in this glycerol conversion process.

In order to understand the reason for the gradual decrease of activity of the catalyst, some characterization were conducted, including $N_2$ adsorption/desorption, XRD, XRF and $NH_3$-TPD. Based on the $N_2$ adsorption/desorption results shown in Table 4, the surface area and pore volume of the catalyst exhibited a decrease from 370 $m^2$ $g^{-1}$ and 0.200 $cm^3$ $g^{-1}$ (fresh catalyst) to 288 $m^2$ $g^{-1}$ and 0.165 $cm^3$ $g^{-1}$ (after five times reaction/regeneration cycles), respectively. This indicated that the pore structure of the catalyst was somewhat collapsed or blocked. To investigate the structure changes of the catalyst before and after regeneration, XRD was also conducted. As shown in Fig. 5, the crystal structure of HZSM-5 changed slightly after regeneration. A decrease in the intensity of the peak at ~8° ($2\theta$) indicated a decrease of crystallinity of HZSM-5.[23,37,38] The XRD patterns also showed a decrease in intensity for the peak at ~24° ($2\theta$), which indicated that aluminum was somehow removed from the framework.[39] To estimate the loss of aluminum, the Si/Al ratio of HZSM-5 was studied by XRF. The Si/Al ratio increased from 25.0 to 27.1 after regeneration, indicating that less than 8 mol% of aluminum was lost after 5 times regeneration. The acid sites of HZSM-5 are important for its activity. The $NH_3$-TPD was used to measure the total acid of HZSM-5 after each reaction/regeneration cycle. As shown in Table 4, the total acid sites of HZSM-5 decreased from 580.6 to 206.2 μmol $g^{-1}$. The great change should be related to the ammonia atmosphere. Based on the above study, the reason for the gradual deactivation of the catalyst was the structural change and the acid site loss. Better catalysts should be developed in a future study.

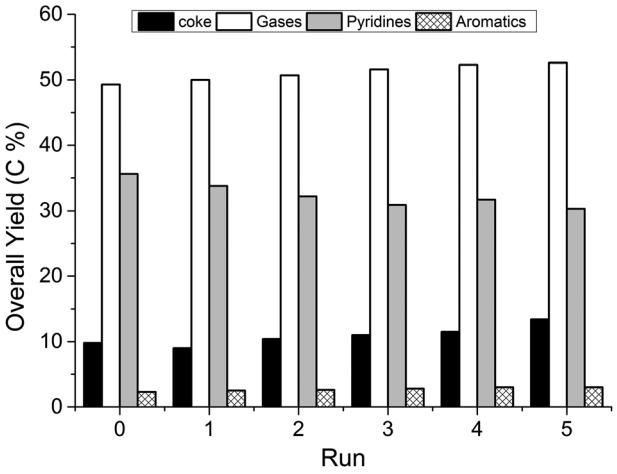


Fig. 4 The recycle of the catalyst recycle. (Reaction conditions: reaction temperature, 550 °C; HZSM-5, Si/Al = 25, 1 g; the WHSV, 1; the $NH_3$ to glycerol molar ratio, 12 : 1; each run was 1 h; glycerol content, 100%.)

Table 4 Typical properties of the catalysts before and after each recycle

| Catalyst | BET surface area ($m^2$ $g^{-1}$) | Pore volume ($cm^3$ $g^{-1}$) | Si/Al[a] | Total acid[b] (μmol $g^{-1}$) |
|---|---|---|---|---|
| HZSM-5-R0 | 370 | 0.200 | 25.0 | 580.6 |
| HZSM-5-R1 | 331.9 | 0.198 | 26.3 | 442.1 |
| HZSM-5-R2 | 312.7 | 0.176 | 26.3 | 363.5 |
| HZSM-5-R3 | 304.4 | 0.172 | 26.4 | 318.2 |
| HZSM-5-R4 | 295.4 | 0.167 | 26.7 | 254.6 |
| HZSM-5-R5 | 288.0 | 0.165 | 27.1 | 206.2 |

[a] Si/Al: the ratio of silicon to aluminum in the zeolites. [b] The detailed $NH_3$-TPD of the recycled catalysts is shown in the supplementary information (Fig. S3).

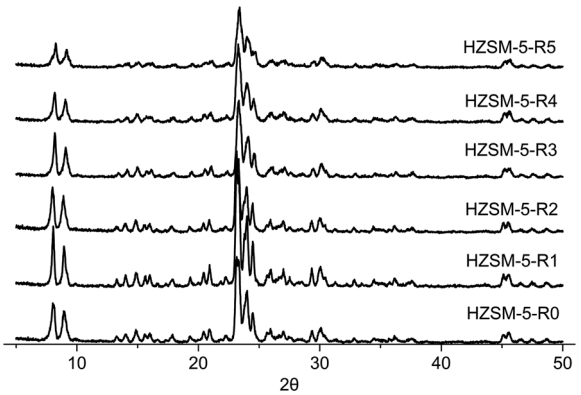


Fig. 5 The X-ray diffraction patterns of the recycled catalysts.

### The reaction pathway of glycerol to pyridines

To further study the pathway from glycerol to pyridines, a series of experiments, such as catalytic dehydration of glycerol under an $N_2$ atmosphere and thermo-catalytic conversion of different oxygenated chemicals which could be formed in the glycerol catalytic dehydration process, were carried out in this study. The detailed product distribution of glycerol catalytic

 

Table 5 Summary of thermo-catalytic conversion of different oxygenated compounds with ammonia for the mechanism study[a]

| | Entry 1 | Entry 2 | Entry 3 | Entry 4 | Entry 5 | Entry 6 | Entry 7 | Entry 8 |
|---|---|---|---|---|---|---|---|---|
| Feedstocks | Glycerol | Acrolein | Acetaldehyde | Acetol | Acetone | Acrolein + acetaldehyde | Acrolein + acetol | Acrolein + acetone |
| Molar ratio | — | — | — | — | — | 1 : 1 | 1 : 1 | 1 : 1 |
| Overall carbon yield (C %) | | | | | | | | |
| Coke | 13.2 | 15.6 | 10.4 | 13.2 | 12.8 | 13.5 | 14.4 | 13.9 |
| Gases | 47.5 | 47.6 | 50.1 | 50.4 | 51.3 | 49.7 | 48.8 | 49.3 |
| Pyridines | 26.0 | 33.7 | 35.9 | 27.6 | 29.4 | 35.0 | 30.5 | 31.6 |
| Aromatics | 0.9 | 2.4 | 2.5 | 2.8 | 2.4 | 2.5 | 2.1 | 2.2 |
| Pyridine selectivity (%) | | | | | | | | |
| Pyridine | 67.3 | 61.2 | 7.6 | 18.8 | 3.0 | 74.3 | 25.0 | 14.9 |
| 2-Methylpyridine | 10.0 | 5.6 | 65.3 | 21.1 | 5.8 | 4.2 | 48.3 | 60.9 |
| 3-Methylpyridine | 21.4 | 33.2 | 1.4 | <1 | 18.9 | 15.1 | 13.8 | 18.2 |
| 4-Methylpyridine | 1.3 | <1 | 25.7 | 9.7 | <1 | 6.4 | 5.6 | <1 |
| Other alkylpyridines[b] | <1 | <1 | <1 | 50.4 | 72.3 | <1 | 7.3 | |

[a] The conversion of different feedstocks was 100%. The reaction temperature was 500 °C. [b] Other alkylpyridines: 2,5-dimethylpyridines, 2,6-dimethylpyridines, 2,4,6-trimethylpyridine *etc*.

dehydration is shown in the ESI (Table S1†). It can be seen that the main feedstocks for pyridine production such as acrolein, acetol, acetaldehyde and acetone could be produced in the glycerol dehydration process. They were employed as the feedstocks for producing pyridines *via* a thermo-catalytic conversion process. The detailed product distribution is shown in Table 5. When acrolein and the mixture of acrolein and acetaldehyde were feedstocks, the product distribution and pyridine selectivity were similar to those of glycerol. Acetaldehyde mainly produced 2-methylpyridine and 4-methylpyridine, while acetol or acetone mainly produced 2,4,6-trimethylpyridine. When the feedstocks were the mixture of acrolein and acetol or acrolein and acetone, the main product in the pyridines was 2-methylpyridine.

Based on all the above investigations, the reaction pathways for the production of pyridines by thermo-catalytic conversion of glycerol with ammonia are proposed and summarized in Fig. 6. Glycerol initially underwent a dehydration process to form acrolein. At the same time, the glycerol also underwent a cracking process to form some other oxygenated chemicals as the by-products, including acetaldehyde, acetol, acetone, *etc*. Then, these oxygenated chemicals reacted with the ammonia

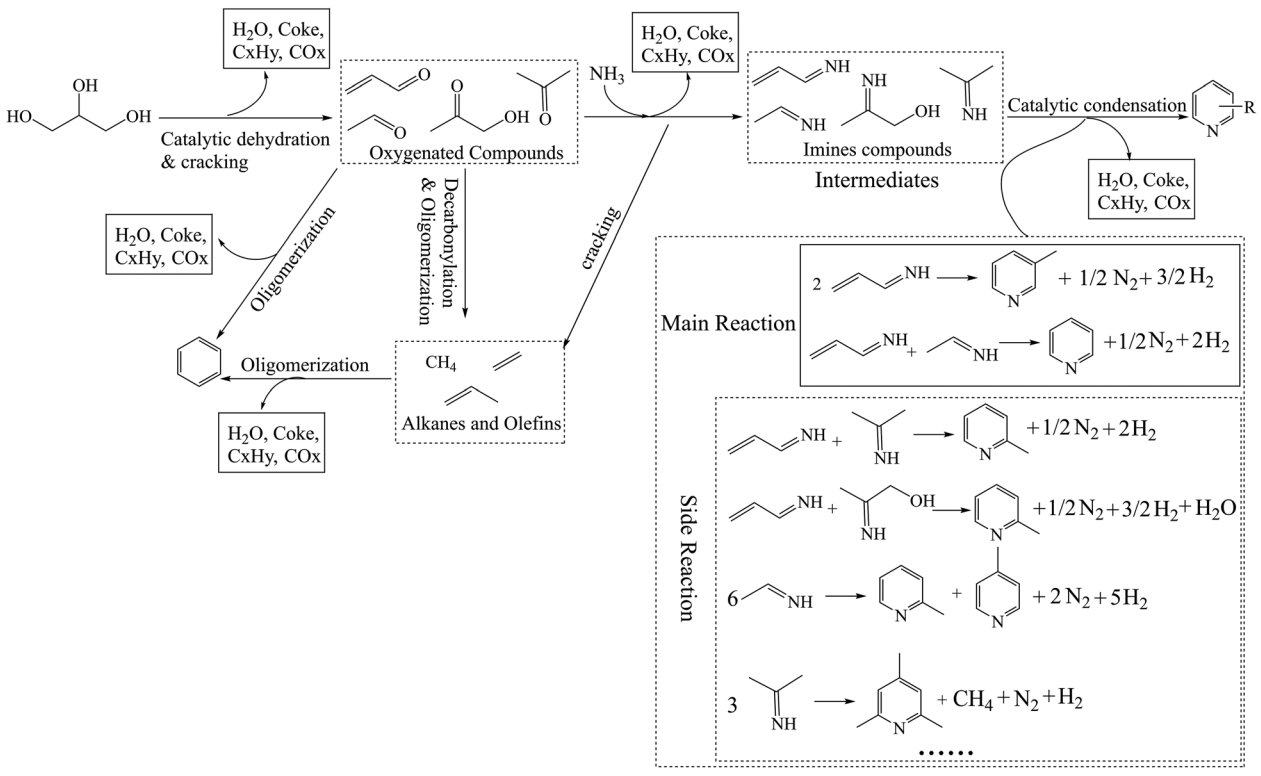


Fig. 6 The proposed reaction pathway from glycerol to pyridines.

to form imine compounds, which were the intermediates in the pyridine production process.[4,9,31] Finally, the imine compounds could be further converted to pyridines *via* the catalytic condensation reaction. According to the product distribution of thermo-catalytic conversion of glycerol and different oxygenated compounds for producing pyridines in Table 5, the reaction of acrolein to pyridines and of the mixture of acrolein and acetaldehyde to pyridines were the main reactions during this process. Meanwhile, certain amounts of coke, $CO_x$, hydrocarbons and $H_2O$ were also formed as the side products during the whole process *via* the decarbonylation, cracking and oligomerization reactions.

## Conclusions

This study demonstrates that pyridines can be synthesized directly from renewable glycerol in the fixed bed reactor over zeolites under an ammonia atmosphere *via* the thermo-catalytic conversion process. In this process, ammonia served not only as the carrier gas, but also as the reactive nitrogen source. Among different catalysts, HZSM-5 with an Si/Al ratio of 25 showed the best reactivity for pyridine production due to the desired pore structure and acidity. Temperature displayed a significant effect on the product distribution. The maximum yield of pyridines was obtained at 550 °C. The WHSV of glycerol to catalyst investigation indicated that a lower WHSV could cause overreaction of glycerol, while a higher WHSV would cause insufficient glycerol conversion to pyridines. The desired WHSV was about 1 $h^{-1}$. Because ammonia served as both a reactant and a carrier gas, to supply sufficient reactants and keep the desired reaction time, an appropriate ammonia to pyridines molar ratio was important on glycerol conversion to pyridines. The addition of water to the feed decreased the pyridine yield, because water competed with glycerol on the acid sites of the catalyst and therefore impacted the acidity of the catalyst. Under optimal conditions, the highest carbon yield of pyridines was 35.6%. After five reaction/regeneration cycles, a slightly irreversible deactivation of the catalyst was observed, which could be due to the structural change and the acid site loss of the catalyst. The reaction pathway from glycerol to pyridines was that glycerol was initially dehydrated to form acrolein and some by-products such as acetaldehyde, acetol, acetone, *etc*., and then acrolein, the mixture of acrolein and acetaldehyde, or other by-products reacted with ammonia to form imines and finally pyridines.

## Acknowledgements

The authors sincerely thank Professor George W. Huber (University of Wisconsin – Madison) for giving valuable suggestions on the experiments and manuscript writing of this work. The authors are also grateful to the National Basic Research Program of China (2013CB228103), NSFC (21325208, 21172209, and 21402181), the Program for Changjiang Scholars and Innovative Research Team in University of the Ministry of Education of China, and the Fundamental Research Funds for the Central Universities (wk 2060190040) for financial support.

## References

1 G. D. Henry, *Tetrahedron*, 2004, **60**, 6043–6061.
2 M. Movassaghi, M. D. Hill and O. K. Ahmad, *J. Am. Chem. Soc.*, 2007, **129**, 10096–10097.
3 K. S. K. Reddy, I. Sreedhar and K. V. Raghavan, *Appl. Catal., A*, 2008, **339**, 15–20.
4 K. S. K. Reddy, C. Srinivasakannan and K. V. Raghavan, *Catal. Surv. Asia*, 2012, **16**, 28–35.
5 S. Shimizu, N. Abe, A. Iguchi, M. Dohba, H. Sato and K. I. Hirose, *Microporous Mesoporous Mater.*, 1998, **21**, 447–451.
6 S. Shimizu, N. Abe, A. Iguchi and H. Sato, *Catal. Surv. Asia*, 1998, **2**, 71–76.
7 J. R. Calvin, R. D. Davis and C. H. McAteer, *Appl. Catal., A*, 2005, **285**, 1–23.
8 F. Jin, F. G. Y. Wu and Y. D. Li, *Chem. Eng. Technol.*, 2011, **34**, 1660–1666.
9 Y. Higashio and T. Shoji, *Appl. Catal., A*, 2004, **260**, 251–259.
10 D. E. Webster and I. M. Rouse, US 4208353 A, 1977.
11 G. A. Renberg, US 3291839 A, 1962.
12 D. Arntz, A. Fischer, M. Höpp, S. Jacobi, J. Sauer, T. Ohara, T. Sato, N. Shimizu and H. Schwind, *Ullmann's Encyclopedia of Industrial Chemistry*, Wiley-VCH, 2012.
13 I. Broder, P. Corey, P. Brasher, M. Lipa and P. Cole, *Environ. Health Perspect.*, 1991, **95**, 101–104.
14 Z. Feng, W. Hu, Y. Hu and M. Tang, *Proc. Natl. Acad. Sci. U. S. A.*, 2006, **103**, 15404–15409.
15 Y. G. Zheng, X. L. Chen and Y. C. Shen, *Chem. Rev.*, 2008, **108**, 5253–5277.
16 B. Katryniok, S. Paul and F. Dumeignil, *ACS Catal.*, 2013, **3**, 1819–1834.
17 L. Z. Tao, B. Yan, Y. Liang and B. Q. Xu, *Green Chem.*, 2013, **15**, 696–705.
18 Y. Nakagawa and K. Tomishige, *Catal. Sci. Technol.*, 2011, **1**, 179–190.
19 N. M. Cullinane, S. J. Chard and R. Meatyard, *J. Chem. Soc., Chem. Ind.*, 1948, **67**, 142–143.
20 L. Z. Tao, S. H. Chai, Y. Zuo, W. T. Zheng, Y. Liang and B. Q. Xu, *Catal. Today*, 2010, **158**, 310–316.
21 Y. Choi, H. Park, Y. Yun and J. Yi, *ChemSusChem*, 2014, DOI: 10.1002/cssc.201402925.
22 A. Corma, G. W. Huber, L. Sauvanaud and P. O'Connor, *J. Catal.*, 2008, **257**, 163–171.
23 Y. T. Kim, K. D. Jung and E. D. Park, *Microporous Mesoporous Mater.*, 2010, **131**, 28–36.
24 S. H. Chai, H. P. Wang, Y. Liang and B. Q. Xu, *Green Chem.*, 2008, **10**, 1087–1093.
25 B. Katryniok, S. Paul, V. Belliere-Baca, P. Rey and F. Dumeignil, *Green Chem.*, 2010, **12**, 2079–2098.

 

26 D. Cespi, F. Passarini, G. Mastragostino, I. Vassura, S. Larocca, A. Iaconi, A. Chieregato, J.-L. Dubois and F. Cavani, *Green Chem.*, 2015, **17**, 343–355.
27 C. H. Zhou, J. N. Beltramini, Y. X. Fan and G. Q. Lu, *Chem. Soc. Rev.*, 2007, **37**, 527–549.
28 X. Li, C. Zhang, C. Qin, C. Chen and J. Shao, CN 101070276, 2007.
29 C. J. Zhou, C. J. Huang, W. G. Zhang, H. S. Zhai, H. L. Wu and Z. S. Chao, *Stud. Surf. Sci. Catal.*, 2007, **165**, 527–530.
30 J. L. Dubois and J. F. Devaux, US 20120283446 A1, 2012.
31 D. Bayramoglu, G. Gurel, *et al.*, *Turk. J. Chem.*, 2014, **38**, 661–670.
32 B. Singh, S. K. Roy, K. P. Sharma and T. K. Goswami, *J. Chem. Technol. Biotechnol.*, 1998, **71**, 246–252.
33 T. R. Carlson, G. A. Tompsett, W. C. Conner and G. W. Huber, *Top. Catal.*, 2009, **52**, 241–252.
34 Q. H. Xia, S. C. Shen and J. Song, *J. Catal.*, 2003, **219**, 74–84.
35 C. T. Kresge, M. E. Leonowicz and W. J. Roth, *Nature*, 1992, **359**, 710–712.
36 M. H. Lim, C. F. Blanford and A. Stein, *J. Am. Chem. Soc.*, 1997, **119**, 4090–4091.
37 T. R. Carlson;, Y. T. Cheng, J. Jae and G. W. Huber, *Energy Environ. Sci.*, 2011, **4**, 145–161.
38 C. H. Ding, X. S. Wang, X. W. Guo and S. G. Zhang, *Catal. Commun.*, 2008, **9**, 487.
39 S. J. Wang, G. W. Guo, L. Q. Zhao and R. H. Wang, *Chin. J. Catal.*, 1992, **13**, 38.